DALTON
FULL PAPER

# Preparation, crystal structures and spectroscopic properties of vanadium(III) complexes with $[V–O–V]^{4+}$ cores †

**Hitoshi Kumagai,[a] Susumu Kitagawa,*[b] Masahiko Maekawa,[c] Satoshi Kawata,[d] Hidenori Kiso[c] and Megumu Munakata[c]**

[a] *Institute for Molecular Science, Myoudaiji, Okazaki, Aichi 444-8585, Japan*
[b] *Graduate School of Engineering, Department of Synthetic Chemistry and Biological Chemistry, Kyoto University, Yoshida, Sakyo-ku, Kyoto 606-8501, Japan*
[c] *Department of Chemistry, Kinki University, Kowakae, Higashi-Osaka, Osaka 577-8502, Japan*
[d] *Department of Chemistry, Shizuoka University, Ohya, Shizuoka 422-8529, Japan*

***Received 20th July 2001, Accepted 13th March 2002***
***First published as an Advance Article on the web 25th April 2002***

Dinuclear vanadium(III) complexes, $[V_2(\mu\text{-O})(phen)_4Cl_2]Cl_2\cdot 2Me_2CO$ (**1**) and $[V_2(\mu\text{-O})(dpya)_4Cl_2]Cl_2$ (**2**) [phen = 1,10-phenanthroline; dpya = bis(2-pyridyl)amine], have been synthesized from the reaction of $VCl_3$ or $VCl_3(THF)_3$ with bidentate nitrogenous ligands. The ligand substitution reaction between NaNCS and **2** yields a brown dinuclear complex, $[V_2(\mu\text{-O})(dpya)_3(NCS)_4]\cdot 2THF$ (**3**), in which each vanadium ion has a different coordination environment, and an orange mononuclear complex, $[V(dpya)(NCS)_4]\cdot(Hdpya)\cdot THF$ (**4**). Complexes **1**–**3** contain singly bridged $[V–O–V]^{4+}$ cores. From the temperature dependence of the magnetic susceptibilities, weak magnetic interactions are observed for **1**–**3**. UV-Vis and resonance Raman spectra of these complexes are described. The $^1H$ NMR spectrum of **1**, in which two vanadium ions are coupled antiferromagnetically, and those of its analogs have been measured and assigned.

## Introduction

Oxo-bridged polynuclear vanadium(III) complexes have been the subject of considerable interest in recent years. Study of these species is motivated by interest in their structural, magnetic and spectroscopic properties.[1] Basic structural motifs for oxo-bridged polynuclear vanadium(III) complexes can be divided into two groups;[2] (1) unsupported, singly bridged μ-oxo species[3–7] and (2) tribridged species in which the oxo-bridge is supported by two co-bridging carboxylate, thiolate or phosphate groups. These include molecules with di-, tri-, octa-[1b,3,8–16] and tetranuclear cores.[17,18] Recent interest in these oxo-bridged vanadium(III) polynuclear complexes has been related to their unusual magnetic and spectroscopic properties.[1b,18] Some divanadium(III) oxo-bridged species show strong ferromagnetic (FM) exchange interactions which switch to antiferromagnetic (AFM) upon protonation of the oxo bridge.[3e,f,11] Another interesting class of oxo-bridged vanadium complexes is tetranuclear vanadium(III) complexes. These exhibit spin frustration effects and/or single-molecule magnet behavior.[17,18]

Although several studies on the structural, magnetic and spectroscopic properties of polynuclear vanadium(III) complexes have been published, only a few attempts have been made to study their reactivity. Oxygen atom transfer and ligand substitution reactions in mononuclear vanadium(III) complexes have been studied.[3d,4,19–21] An oxo-bridged vanadium(III) dimer has been isolated as an intermediate of the oxygen atom transfer reaction.[3d,19,20] Substitution reactions at the V–Cl bond have also been studied, since the chloride ions are quite labile.[4,21,22] Although the nature of the substituent influences the redox potential of the metal, which can be an electron donor to a variety of substrates,[21] only a few attempts have so far been made to study ligand substitution reactions of monobridged dinuclear vanadium(III) complexes with X-ray crystallographic characterization of the reaction products. The singly bridged dinuclear vanadium(III) complex described here has two V–Cl bonds which may be substituted. Our interest in the substitution reaction is primarily directed towards the structure and properties of the products.

In addition to single-crystal X-ray structural information, the characterization of singly bridged dinuclear vanadium(III) complexes in solution is of use for the investigation of their structural and bonding properties in the solution state.[23–25] Spectroscopic techniques, including UV-Vis and resonance Raman spectroscopies, have been applied previously to the investigation of these properties.[2,3,26,27] While the $^1H$ NMR spectra of tribridged species have been measured before,[1b,8,15,28] NMR data for singly bridged species are scarce.[29] We have, therefore, obtained the $^1H$ NMR spectra for the antiferromagnetically coupled system and discuss the interaction between the two vanadium ions.

Herein, we describe the synthesis and crystal structures of novel singly bridged dinuclear vanadium(III) complexes and a substitution product with two types of vanadium environments within the molecule, together with its spectroscopic and magnetic properties.

## Experimental

All manipulations were carried out using standard Schlenk techniques. Solvents were purified by standard methods before use. 1,10-Phenanthroline (1,10-phen), 4,7-dimethyl-1,10-phenanthroline (4,7-$Me_2$phen), 5,6-dimethyl-1,10-phenanthroline (5,6-$Me_2$phen) and 3,4,7,8-tetramethyl-1,10-phenanthroline (3,4,7,8-$Me_4$phen) were purchased from Tokyo Kasei Co. $VCl_3$, sodium thiocyanate and bis(2-pyridyl)amine (dpya) were purchased from Aldrich Chemical Co. and used without further purification. $VCl_3(THF)_3$ was prepared according to the literature method.[30] IR spectra were measured using KBr disks

† Electronic supplementary information (ESI) available: $^1H$ NMR spectrum of complex **1**. See http://www.rsc.org/suppdata/dt/b1/b106517n/

 DOI: 10.1039/b106517n

on a Hitachi I-5040-FT IR spectrometer. Raman spectra were measured with $Ar^+$ ion excitation using a JASCO R600 spectrometer. A 90° scattering geometry was employed. UV-Vis spectra were recorded on a Hitachi U-3500 spectrophotometer. EPR spectra were recorded at X-band frequency with a modulation frequency of 100 kHz and a modulation amplitude of 1 mT using a JEOL RE-3X spectrometer. Resonance frequencies were measured on an Anritsu MF76A microwave frequency counter. Magnetic fields were calibrated by an ECHO Electronics EF 2000AX NMR field meter. NMR spectra were measured with a JEOL GSX-270 FT-NMR spectrometer or an EX-400 FT-NMR spectrometer. Variable temperature magnetic susceptibility data were recorded over the temperature range 3 to 300 K using a Quantum Design SQUID susceptometer interfaced with an HP Vectra computer system. All data were corrected for diamagnetism, which was calculated from Pascal's table.

### Preparation of $[V_2(\mu\text{-}O)(phen)_4Cl_2]Cl_2\cdot 2Me_2CO$ (1)

$VCl_3$ (62 mg, 0.4 mmol) was dissolved in 4 ml of ethanol. To this solution, phen (0.2 g, 1.2 mmol) in ethanol was added. The solution mixture was stirred and a violet colored solution was obtained. Acetone was diffused slowly into this solution until violet crystals of **1** were obtained (yield 42%). Anal. found: C, 57.89; H, 4.14; N, 10.22%. Calcd for $V_2O_3C_{54}N_8Cl_4H_{44}$: C, 59.14; H, 4.04; N, 10.22%.

Other vanadium complexes of phen derivatives were synthesized *via* procedures similar to that used for the preparation of **1**.

### Preparation of $[V_2(\mu\text{-}O)(dpya)_4Cl_2]Cl_2$ (2)

$VCl_3(THF)_3$ (0.3 g, 0.8 mmol) was dissolved in 4 ml of ethanol and an ethanolic solution of dpya (0.27 g, 1.6 mmol) was added. The solution mixture was stirred and a violet solution was obtained. After stirring for two hours, acetone was allowed to diffuse into the obtained violet solution. Violet crystals of **2** were formed within a month (yield 65%). Anal. found: C, 46.47; H, 4.04; N, 16.10%. Calcd for $V_2OC_{40}N_{12}Cl_4H_{36}$: C, 50.87; H, 3.84; N, 17.80%. Raman ($cm^{-1}$) 1290, 648, 411.

### Preparation of $[V_2(\mu\text{-}O)(dpya)_3(NCS)_4]\cdot 2THF$ (3) and $[V(dpya)(NCS)_4]\cdot(Hdpya)\cdot THF$ (4)

A suspension of sodium thiocyanate (0.09 g, 2.4 mmol) in 4 ml of THF was added to the violet solution prepared as described for **2**. The color changed from violet to brown. The mixture was stirred and filtered to remove NaCl. THF was layered slowly on the resulting brown solution. Air and moisture sensitive brown crystals of complex **3** and orange crystals of complex **4** were obtained within two weeks. These crystals were separated mechanically. The yields could not be calculated. Anal. found (for complex **3**): C, 48.45; H, 4.35; N, 18.19%. Calcd for $V_2O_3C_{42}N_{13}S_4H_{43}$: C, 50.05; H, 4.30; N, 18.06%. Raman ($cm^{-1}$) 1327, 1244, 1156, 662 for **3** and 1240 and 1150 for **4**. IR $\nu$(C–N)/$cm^{-1}$: 2069 for **3** and 2046 for **4**.

### X-Ray crystallography and structure solution

Data for complex **1** was collected on a Rigaku AFC5R. Complexes **3** and **4** were collected on a Rigaku AFC7R. Both diffractometers employ graphite monochromated Mo-Kα radiation. The data were collected at room temperature. An empirical absorption correction was applied. The data were corrected for Lorentz and polarization effects. The structure was solved by direct methods and expanded using Fourier techniques.[32] The non-hydrogen atoms were refined anisotropically. The final cycle of full-matrix least-squares refinement was based on the number of observed reflections [$I > 3.00\sigma(I)$] and $n$ variable parameters, and converged (large parameter shift was $\sigma$ times its e.s.d.) with weighted and unweighted agreement factors of $R = \Sigma||F_o| - |F_c||/\Sigma|F_o|$, $Rw = [\Sigma w(|F_o| - |F_c|)^2/\Sigma w|F|_o^2]^{1/2}$. No extinction corrections have been applied.

For complexes **1** and **3**, a crystal was mounted in a glass capillary to avoid oxidation and loss of solvent molecules of crystallization. Over the course of data collection, the standard reflections decreased by −19.9% (**3**). A linear correction factor was applied to the data to account for this phenomenon. For complexes **3** and **4**, the thermal parameters for the solvent molecules indicate the presence of disorder. Crystallographic data is given in Table 1.

CCDC reference numbers 167774, 167776 and 167777.

See http://www.rsc.org/suppdata/dt/b1/b106517n/ for crystallographic data in CIF or other electronic format.

## Results and discussion

### The structure of 1

The structure of $[V_2(\mu\text{-}O)(phen)_4Cl_2]^{2+}$ with a singly bridged V–O–V moiety is shown in Fig. 1. Oxygen atom O(1) lies on a

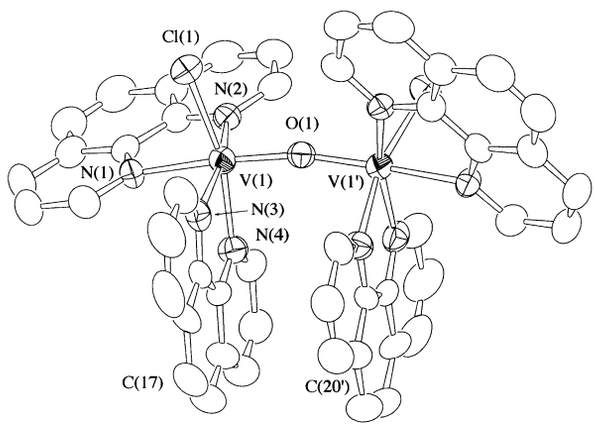


**Fig. 1** ORTEP drawing of $[V_2(\mu\text{-}O)(phen)_4Cl_2]^{2+}$ (**1**), showing the atom-labeling scheme, with thermal ellipsoids at the 50% probability level. Hydrogen atoms are omitted for clarity.

two-fold crystallographic axis and the cation thus has 2-fold imposed symmetry. Selected bond lengths and angles are given in Table 2. The bond angles and distances observed for complex **1** indicate that the geometry is quite similar to that found in the previously reported structure of $[V_2O(phen)_4Cl_2]Cl_2\cdot 8H_2O$, containing water molecules in the crystal lattice.[5] The octahedral coordination around the vanadium(III) atom is composed of the bridging oxo group, the nitrogen atoms of the phen ligand and the chloride ion, to afford a $VON_4Cl$ coordination environment. The V–N distances are similar to those found in complexes of pyridine derivatives.[3,6] The $V\text{–}O_{oxo}$ distances in complex **1** [1.778(2) Å] are in the range of those found in other singly bridged dinuclear vanadium complexes.[2–7,33–39] It appears to be a general trend among vanadium complexes that the vanadium to ligand distances do not vary with changes in the formal oxidation state.[33] The V(1)–N(1) distance [2.183(7)Å] is lengthened due to the *trans* influence of the bridging oxo group. The *trans* influence of the bridging oxo group has been observed in other oxo-bridged dinuclear vanadium(III) complexes.[3]

Although a few complexes exhibit small V–O–V angles,[39,40] most of the V–O–V angles for crystallographically characterized complexes fall within the range 180 to 173.5(3)°.[2–7,29] Despite the fact that complex **1** contains acetone molecules instead of water molecules, it crystallizes in the same space group. Complex **1** also exhibits characteristic π–π stacking interactions between the nearly parallel phen rings [nearest neighbor C(17)–C(20′) distance: 3.37 Å].[5] The π–π stacking interaction decreases the V–O–V angle in complex **1** [168.0(5)°].

**Table 1** Summary of crystal data and experimental parameters for the X-ray crystallographic studies of $[V_2(\mu\text{-}O)(phen)_4Cl_2]Cl_2\cdot 2Me_2CO$ (**1**), $[V_2(\mu\text{-}O)(dpya)_3(NCS)_4]\cdot 2THF$ (**3**) and $[V(dpya)(NCS)_4]\cdot(Hdpya)\cdot THF$ (**4**)

| Complex | **1** | **3** | **4** |
|---|---|---|---|
| Empirical formula | $VCl_2ON_4C_{27}H_{22}$ | $V_2O_3C_{42}N_{13}S_4H_{43}$ | $VOC_{28}N_{10}S_4H_{27}$ |
| Formula weight | 548.34 | 1008.01 | 698.77 |
| Crystal system | Orthorhombic | Monoclinic | Triclinic |
| Space group | *Pbcn* | $P2_1/n$ | $P\bar{1}$ |
| *a*/Å | 18.209(8) | 16.980(2) | 13.331(3) |
| *b*/Å | 10.673(3) | 17.057(4) | 17.890(2) |
| *c*/Å | 25.087(8) | 18.199(2) | 8.405(1) |
| *α*/° | | | 93.41(1) |
| *β*/° | | 103.592(9) | 91.08(1) |
| *γ*/° | | | 107.11(1) |
| *V*/Å$^3$ | 4876(5) | 5123(1) | 1911.2(5) |
| *Z* | 8 | 4 | 2 |
| $D_c$/g cm$^{-3}$ | 1.494 | 1.307 | 1.214 |
| $\mu$(Mo-K$\alpha$)/cm$^{-1}$ | 6.44 | 5.77 | 5.12 |
| *F*(000) | 2248.00 | 2080.00 | 720 |
| $\theta$ range (max.) | 24.98 | 27.56 | 27.56 |
| *hkl* range | $0 < h < 19$ | $0 < h < 22$ | $0 < h < 17$ |
| | $0 < k < 12$ | $0 < k < 22$ | $-23 < k < 22$ |
| | $-29 < l < 0$ | $-23 < l < 23$ | $-10 < l < 10$ |
| No. observations [$I > 3.00\sigma(I)$] | 1535 | 4596 | 3407 |
| No. variables | 321 | 532 | 368 |
| *R* | 0.057 | 0.080 | 0.100 |
| *Rw* | 0.070 | 0.101 | 0.158 |

**Table 2** Selected bond distances (Å) and angles (°) for **1**

| | | | |
|---|---|---|---|
| V(1)–O(1) | 1.778(2) | V(1)–Cl(1) | 2.351(3) |
| V(1)–N(1) | 2.183(7) | V(1)–N(2) | 2.103(8) |
| V(1)–N(3) | 2.119(8) | V(1)–N(4) | 2.118(8) |
| | | | |
| Cl(1)–V(1)–O(1) | 101.3(3) | Cl(1)–V(1)–N(1) | 88.1(2) |
| Cl(1)–V(1)–N(2) | 89.8(2) | Cl(1)–V(1)–N(3) | 94.3(3) |
| Cl(1)–V(1)–N(4) | 165.7(2) | O(1)–V(1)–N(1) | 167.5(2) |
| O(1)–V(1)–N(2) | 95.2(3) | O(1)–V(1)–N(3) | 97.7(3) |
| O(1)–V(1)–N(4) | 90.9(3) | N(1)–V(1)–N(2) | 76.4(3) |
| N(1)–V(1)–N(3) | 89.8(3) | N(1)–V(1)–N(4) | 81.0(3) |
| N(2)–V(1)–N(3) | 165.5(3) | N(2)–V(1)–N(4) | 96.4(3) |
| N(3)–V(1)–N(4) | 76.6(3) | V(1)–O(1)–V(1′) | 168.0(5) |

The X-ray structural analyses of $[V_2O(L\text{-his})_4]\cdot 2H_2O$ (L-his = L-histidinate)[2,3a] and $[V_2O(phen)_4Cl_2]Cl_2\cdot 8H_2O$[5] reveal unusually small bent angles of 153.9(2) and 169.6(3)°, respectively, due to the intramolecular hydrogen bonding interaction of L-his and π–π stacking interactions between the ligands. The V–O–V angle is flexible and easily distorted in response to a number of weak interactions, such as π–π stacking and hydrogen bonding.[2,3a,d,5] The planar phen rings of complex **1** show bond-over-ring π–π stacking interactions.

### The structure of 3

The X-ray crystal structure of complex **3** reveals the presence of a neutral dinuclear $[V_2(\mu\text{-}O)(dpya)_3(NCS)_4]$ complex with three well-separated THF molecules of crystallization. The molecular structure of the complex $[V_2(\mu\text{-}O)(dpya)_3(NCS)_4]$ is shown in Fig. 2. Selected bond lengths and angles are given in Table 3. The molecule is a singly bridged dinuclear vanadium(III) complex. Each vanadium(III) atom is in a pseudooctahedral environment comprising dpya ligands, thiocyanato ligands and a bridging oxygen atom ($VON_5$ coordination sphere). The V–O–V angle of complex **3** [173.6(4)°] is in the same range as those found in other singly bridged vanadium(III) complexes.[2–7,29] It is worth noting from Fig. 2 that each vanadium(III) atom has different donor ligands. While terminal ligation at the V(1) atom is provided by one thiocyanato ligand and two dpya ligands, the V(2) atom is coordinated by one dpya ligand and three thiocyanato ligands. This asymmetric dinuclear complex is a unique example among crystallographically characterized vanadium(III) complexes. The $V–O_{oxo}$ distances of 1.771(6) and 1.778(6) Å are comparable with those of complex **1** and other

**Table 3** Selected bond distances (Å) and angles (°) for **3**

| | | | |
|---|---|---|---|
| V(1)–O(1) | 1.778(6) | V(1)–N(1) | 2.118(8) |
| V(1)–N(3) | 2.182(8) | V(1)–N(4) | 2.128(8) |
| V(1)–N(6) | 2.128(8) | V(1)–N(7) | 2.041(9) |
| V(2)–O(1) | 1.771(6) | V(2)–N(8) | 2.135(9) |
| V(2)–N(10) | 2.126(8) | V(2)–N(11) | 2.055(9) |
| V(2)–N(12) | 2.048(9) | V(2)–N(13) | 2.079(9) |
| | | | |
| O(1)–V(1)–N(1) | 93.7(3) | O(1)–V(2)–N(8) | 91.4(3) |
| O(1)–V(1)–N(3) | 175.3(3) | O(1)–V(2)–N(10) | 90.4(3) |
| O(1)–V(1)–N(4) | 92.3(3) | O(1)–V(2)–N(11) | 96.0(3) |
| O(1)–V(1)–N(6) | 93.4(3) | O(1)–V(2)–N(12) | 94.1(3) |
| O(1)–V(1)–N(7) | 96.7(3) | O(1)–V(2)–N(13) | 175.1(3) |
| N(1)–V(1)–N(3) | 82.6(3) | N(8)–V(2)–N(10) | 83.9(3) |
| N(1)–V(1)–N(4) | 90.9(3) | N(8)–V(2)–N(11) | 171.5(4) |
| N(1)–V(1)–N(6) | 172.2(3) | N(8)–V(2)–N(12) | 93.1(4) |
| N(1)–V(1)–N(7) | 91.9(3) | N(8)–V(2)–N(13) | 84.8(3) |
| N(3)–V(1)–N(4) | 84.9(3) | N(10)–V(2)–N(11) | 91.7(3) |
| N(3)–V(1)–N(6) | 90.2(3) | N(10)–V(2)–N(12) | 174.6(4) |
| N(3)–V(1)–N(7) | 86.4(3) | N(10)–V(2)–N(13) | 86.0(3) |
| N(4)–V(1)–N(6) | 85.5(3) | N(11)–V(2)–N(12) | 90.7(4) |
| N(4)–V(1)–N(7) | 170.4(3) | N(11)–V(2)–N(13) | 87.6(3) |
| N(6)–V(1)–N(7) | 90.6(3) | N(12)–V(2)–N(13) | 89.3(4) |
| V(1)–O(1)–V(2) | 173.6(4) | | |

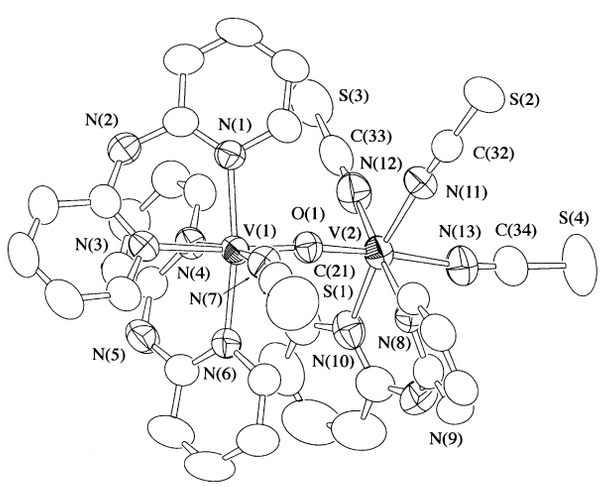


**Fig. 2** ORTEP drawing of $[V_2(\mu\text{-}O)(dpya)_3(NCS)_4]$, showing the atom-labeling scheme, with thermal ellipsoids at the 50% probability level. Hydrogen atoms are omitted for clarity.

**Table 4** Selected bond distances (Å) and angles (°) for **4**

| | | | |
|---|---|---|---|
| V(1)–N(1) | 2.098(8) | V(1)–N(3) | 2.099(8) |
| V(1)–N(4) | 2.011(10) | V(1)–N(5) | 2.028(9) |
| V(1)–N(6) | 2.03(1) | V(1)–N(7) | 2.01(1) |
| N(1)–V(1)–N(3) | 83.1(3) | N(3)–V(1)–N(4) | 174.8(4) |
| N(1)–V(1)–N(4) | 92.0(3) | N(3)–V(1)–N(5) | 91.2(3) |
| N(1)–V(1)–N(5) | 174.3(3) | N(3)–V(1)–N(6) | 89.9(3) |
| N(1)–V(1)–N(6) | 88.7(3) | N(3)–V(1)–N(7) | 88.1(3) |
| N(1)–V(1)–N(7) | 89.0(4) | N(5)–V(1)–N(6) | 91.0(4) |
| N(4)–V(1)–N(5) | 93.7(4) | N(5)–V(1)–N(7) | 91.2(4) |
| N(4)–V(1)–N(6) | 91.7(4) | N(6)–V(1)–N(7) | 177.1(4) |
| N(4)–V(1)–N(7) | 90.1(4) | | |

related crystallographically characterized complexes.[2–7,33–39] The V(1)–N(3) bond distance [2.182(8) Å] is longer (0.06 Å) than the other V–$N_{dpya}$ distances due to the *trans* influence of the bridging oxo group. The V(2)–N(13) bond [2.079(9) Å] of the thiocyanato ligand in the *trans* position with respect to the bridging oxygen is very similar in length to the V(2)–$N_{NCS}$ bonds [2.055(9) and 2.048(9) Å]. The structural influence of the μ-oxo group is also observed in complex **3** (V–$N_{NCS}$ bond lengthened by 0.03 Å). The relatively small *trans* influence on the V–$N_{NCS}$ distance is due to anionic character of the $NCS^-$ ligand. This *trans* influence has also been observed in other crystallographically characterized oxo-bridged dinuclear complexes.[2,3] The V(1)–$N_{NCS}$ bond distance [2.041(9) Å] is shorter than the V(2)–$N_{NCS}$ distances in **3**.

### The structure of 4

The crystal structure of complex **4** reveals the presence of two THF molecules and a metal-free $Hdpya^+$ as the counter ion of the $[V(dpya)(NCS)_4]^-$ anion. The structure of $[V(dpya)(NCS)_4]^-$, with the atomic numbering scheme, is given in Fig. 3.

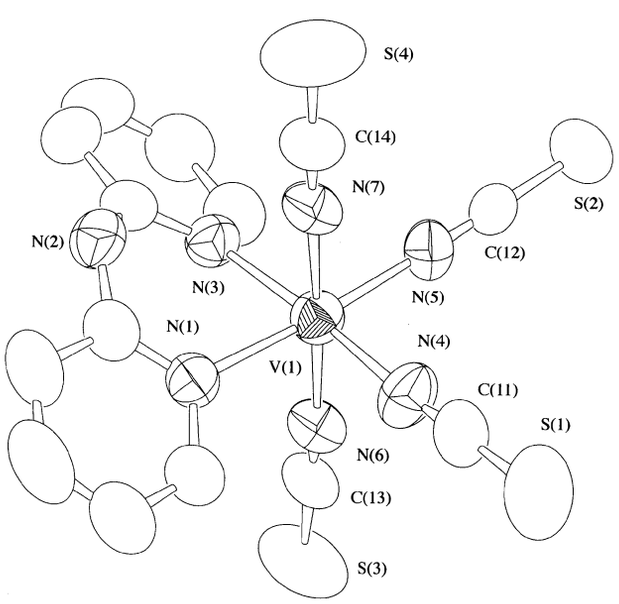


**Fig. 3** ORTEP drawing of $[V(dpya)(NCS)_4]^+$, showing the atom-labeling scheme, with thermal ellipsoids at the 50% probability level. Hydrogen atoms are omitted for clarity.

Selected bond distances and angles for complex **4** are shown in Table 4. THF molecules of crystallization are hydrogen bonded to the $Hdpya^+$ cations and coordinated dpya. The vanadium atom shows a slightly distorted octahedral geometry with a $VN_6$ donor environment. The V–$N_{dpya}$ distances and chelate angle are 2.098(8) and 2.099(8) Å, and 83.1(3)°, respectively. Both complexes **3** and **4** contain the same $[V(dpya)(NCS)_3]$ unit. The bond distances of the $[V(dpya)(NCS)_3]$ unit in complex **4** are shorter than those found in **3**. This difference is associated with the bridging oxo group.

### The reactions of 2

The reaction between $VCl_3(THF)_3$ and dpya affords violet crystals of $[V_2(\mu\text{-}O)(dpya)_4Cl_2]Cl_2$ (**2**). Even when a crystal of **2** was mounted in a glass capillary, it readily decomposed. However, we did manage to determine an outline view of the μ-oxo dinuclear structure. **2** crystallizes in a monoclinic unit cell with $a = 35.158(8)$, $b = 16.984(4)$, $c = 20.180(8)$ Å, $\beta = 112.09(3)°$, $V = 11165(5)$ Å$^3$, space group $C2/c$.[41] This structure is consistent with UV-Vis and Raman spectroscopic measurements. Substitution of the chloride ions by thiocyanate changes the color of the solution from violet to brown. Sodium salts of thiocyanate, azide and cyanate have been used in reactions with mononuclear vanadium(III) and vanadium(IV) complexes.[4,21,22] Because complexes **3** and **4** are unstable in air, we could not obtain good elemental analyses. However, based on the X-ray crystallographic studies, we can identify the reaction products as two vanadium(III) species, which are the μ-oxo dinuclear complex **3** and the mononuclear complex **4**. As shown in Scheme 1, there are two types of dpya coordination with respect to the bridging oxo group in complex **2**. The first example displays *cis–cis* (type A) coordination of the pyridyl groups. The second example is *cis–trans*(type B) coordination of the pyridyl group with respect to the bridging oxo group. The thiocyanate ligands substitute not only the two chloride ligands but also one dpya coordinated in the *trans* position. For complex **3**, a dpya (type B) is selectively substituted due to the *trans* effect of the bridging μ-oxo group, and the $[V–O–V]^{4+}$ core is retained during the substitution reaction. However, the reason why only one half of the type B ligand is replaced is not clear at this stage.

### Magnetic properties

Powdered samples of **1**, **2** and **4** gave no EPR spectra both at room and liquid nitrogen temperatures. In octahedral environments, vanadium(III) complexes have an orbital triplet ground state and spin–orbit coupling is operative to give large zero-field splitting and short spin-lattice relaxation times, which make EPR spectra undetectable.[31,42,43] Only in a special case has the vanadium(III) state has been detected by EPR spectroscopy at low temperature.[44,45] Thus, it is reasonable to assume that complexes **1**, **2** and **4** are formally trivalent.

Variable temperature magnetic susceptibility studies have been performed on powdered samples of μ-oxo vanadium(III) dimers over the temperature range 9 to 172 K for **1** and from 3 to 300 K for **2** and **3**. The effective magnetic moment of complex **1** was measured in solution, and an Evans NMR determination of its magnetic moment in $CD_3OD$ yielded a value of 3.24 $\mu_B$ per vanadium at room temperature. The effective magnetic moments of solid samples of **2** and **3** at 300 K are 3.19 and 3.31 $\mu_B$ per vanadium, respectively, which are larger than the spin-only value of 2.83 $\mu_B$ per vanadium for an octahedral vanadium(III) complex. The effective magnetic moments of these complexes decrease at lower temperature (2.28 and 2.91 $\mu_B$ per vanadium at 3 K for **2** and **3**, respectively). These complexes exhibit similar Curie–Weiss behavior, with $\theta$ = −3.69, −1.58 and −1.62 K for complexes **1**, **2** and **3**, respectively. This behavior is indicative of weak antiferromagnetic interaction between the vanadium(III) ($d^2$) ions. A reasonable fit to the data was not obtained by using the isotropic exchange Hamiltonian $H = -2JS_1 \cdot S_2$, where $S_1 = S_2 = 1$ for the vanadium(III) dimer without a zero-field splitting constant. As a result of a weak magnetic interaction, the $J$ values of these complexes are comparable to the zero-field splitting constant. Consequently, it is difficult to analyze the temperature dependence of the magnetic susceptibility using an isotropic exchange Hamiltonian without a zero-field splitting constant.

Singly oxo-bridged dinuclear vanadium(III) compounds exhibit variations in magnetic behavior. **1**–**3** show intramolecular antiferromagnetic interactions, as does $[V_2O(bpy)_4Cl_2]Cl_2$ (3.17 $\mu_B$ per vanadium, $\theta = -0.64$).[6] $[V_2O(SCH_2CH_2$-

**Table 5** Spectroscopic properties of (μ-oxo) dinuclear complexes[a]

| Complexes | V–O–V angle/° | Electronic spectrum/nm | Raman bands [$2\nu_{as}$(V–O–V)/cm$^{-1}$] | Coordination environment | Ref. |
|---|---|---|---|---|---|
| $[V_2O(SCH_2CH_2NMe_2)_4]$ | 177.84(25) | 463 | | $ON_2S_2$ | 7 |
| $[V(BH_4)_2(PMe_3)_2]_2(O)$ | 178.7(1) | | | $OH_4P_2$ | 29 |
| $[V_2OCl_4(THF)_6]$ | 180 | 482 | | $O_4Cl_2$ | 3*d* |
| $[V_2OCl_4(py)_6]$ | 180, 178.7(8) | 538 | | $ON_3Cl_2$ | 19 |
| $[L_2V_2(acac)_2(O)]I_2$ | 180 | 539 | | $O_3N_3$ | 3*c* |
| $[V_2$(L-his)$_4(O)]$ | 153.9(2) | 478.5 | 1437 | $O_2N_4$ | 2, 3*a* |
| $[\{VBr(tpa)\}_2(O)]$ | 175.3(2) | 540 | 1324 | $ON_4Br$ | 4 |
| $[\{VCl(bpy)_2\}_2O]Cl_2$ | 173.5 | 546, 656 | | $ON_4Cl$ | 6 |
| $[\{VCl(phen)_2\}_2O]Cl_2$ | 168.0(5), 169.6(3) | 480(sh), 542, 662 | | $ON_4Cl$ | This work, 5 |
| $[V_2(dpya)_3(NCS)_4\}_2O]$ | 173.6(4) | 538, 614 | 1327 | $ON_5$ | This work |

[a] L = 1,4,7-trimethyl-1,4,7-triazacyclononane, L-his = L-histidinate, tpa = tetrapyridylamine.

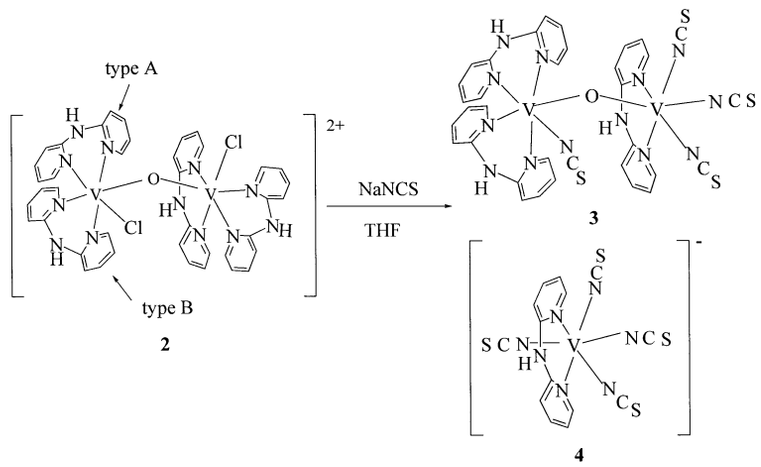


**Scheme 1**

$NMe_2)_4$] exhibits no appreciable superexchange interaction,[7] possibly because of its five-coordinate geometry.[4] Intramolecular ferromagnetic spin–exchange coupling ($S = 2$ ground state) is also found in $[L_2V_2(acac)_2(\mu\text{-}O)]I_2{\cdot}2H_2O$ and $[V_2(\mu\text{-}O)\text{-}Br_2(tpa)_2]Br$ (L = 1,4,7-trimethyl-1,4,7-triazacyclononane, tpa = tetrapyridylammonium ion).[3c,4]

## Spectroscopic properties

Spectroscopic data for all the singly bridged dinuclear vanadium(III) systems synthesized and characterized by X-ray crystallography to date are listed in Table 5. The electronic spectra of all the oxo-bridged complexes display intense absorption maxima ($\varepsilon > 3000$ M$^{-1}$ cm$^{-1}$) in the visible region: 480(sh), 542 and 662 nm for **1**, 548 and 634 nm for **2**, 538 and 614 nm for **3**. It has been recognized that complexes containing linear $[V–O–V]^{4+}$ cores exhibit an intense absorption maximum in the visible region.[46] The absorption band is due to a ligand-to-metal charge transfer (LMCT, μ-$O^{2-}$ to $V^{3+}$) band of the $[V–O–V]^{4+}$ unit.[3a,26]

Raman spectra of powdered samples of **2**–**4** in KBr pellets were measured. Both complexes **3** and **4** show Raman bands at ~1240 and ~1150 cm$^{-1}$ attributed to ν(NCS). The Raman bands at 1290 and 1327 cm$^{-1}$ can be assigned to the $2\nu_{as}$(V–O–V) of binuclear complex **2** and **3**, respectively. In the case of complex **1**, the antisymmetric V–O–V stretching band was hardly observed because of the weak intensity. Resonance Raman spectroscopic investigations for oxo-bridged dinuclear vanadium(III) complexes have been studied.[1b,2,3a,b,26,47] While the $2\nu_{as}$(V–O–V) bands for several singly bridged dinuclear vanadium(III) complexes having an aminopolycarboxylato ligand are observed near 1500 cm$^{-1}$,[3c] the $2\nu_{as}$(V–O–V) bands of complexes **2** and **3** is found at significantly lower frequencies. It has been found that $2\nu_{as}$(V–O–V) increases as the energy of the oxo to vanadium(III) charge-transfer transition increases for singly bridged dinuclear vanadium(III) complexes.[13] Coordination of bromide, pyridyl nitrogen and imidazolyl nitrogen decreases the energy of the V–O–V stretching and the LMCT transition.[3c] As can be seen in Table 5, the $ON_4X$ (X = Cl or Br) and $ON_5$ chromophores of the singly bridged $[V–O–V]^{4+}$ cores exhibit intense absorption maxima in the visible region (*ca.* 540 nm) and show $2\nu_{as}$(V–O–V) bands at *ca.* 1300 cm$^{-1}$ in their Raman spectra. This result indicates that the $NCS^-$ group exhibits the same influence on the energy of V–O–V stretching and the LMCT transition.

## $^1$H NMR spectra

In order to examine the vanadium species in solution, their $^1$H NMR spectra were obtained. The $^1$H NMR signals of mononuclear paramagnetic vanadium(III) complexes are often broadened. On the other hand, when two vanadium(III) ions are close to each other, so that antiferromagnetic interaction occurs, their $^1$H NMR signals can be observed, due to the narrowing of isotropic shifts and linewidths.[23,25]

Complex **1** gave eight broad $^1$H NMR signals in the region 45 to −40 ppm ($\Delta\nu_{1/2}$ = 200 to 2000 Hz), illustrating that the effective antiferromagnetic interaction in solution is maintained, as it is in the solid state (see ESI). The eight signals can be classified in two groups according to the linewidths: the broader four signals, denoted by (B) are shifted to a greater degree than the narrower ones (A). Crystallographic studies (Fig. 1) indicate the existence of *cis*-phen and *trans*-phen around the bridging O atom. The superexchange interaction of spins on the vanadium(III) dπ orbitals occurs through the pπ orbital of the O bridge and the transmission of spin densities on *cis*- and *trans*-phen could be different for **1**. Therefore, the two types of signals, A and B, are attributed to *cis*- and *trans*-positions. However, further assignment of the signals A or B to *cis*- or *trans*-phen is beyond the scope of this experiment.[24,48] The

**Table 6** Observed $^1$H NMR chemical shifts and linewidths at half height for dinuclear vanadium(III) complexes

| | $\delta^a$/ppm ($\Delta\nu_{1/2}$/Hz) | | | | | | | |
|---|---|---|---|---|---|---|---|---|
| | 3,8-H (A)[b] | 3,8-H (B) | 5,6-H (A) | 5,6-H (B) | 2,9-H (A) | 2,9-H (B) | 4,7-H (A) | 4,7-H (B) |
| $[V_2Cl_2(phen)_4(\mu\text{-}O)]Cl_2$ (**1**) | 17.5 (570) | 37.2 (1350) | 7.5 (290) | 13.6 (200) | 4.1 (250) | −2.1 (300) | −17.2 (950) | −32.7 (2100) |
| $[V_2Cl_2(4,7\text{-}Me_2phen)_4(\mu\text{-}O)]Cl_2$ | 18.8 (1200) | 35.0 (1650) | 6.8 | 13.0 (450) | —[c] | −2.3 (525) | 32.9 (Me) (1350) | 50.4 (Me) (1500) |
| $[V_2Cl_2(3,4,7,8\text{-}Me_4phen)_4(\mu\text{-}O)]Cl_2$ | −10.5 (Me) (825) | −25.6 (Me) (1575) | 7.2 (300) | 13.3 (300) | −2.8 (525) | −12.6 (825) | 31.9 (Me) (1350) | 49.5 (Me) (1800) |
| $[V_2Cl_2(5,6\text{-}Me_2phen)_4(\mu\text{-}O)]Cl_2$ | 17.5 (825) | 37.5 (1950) | −1.7 (Me) (150) | −7.3 (Me) (300) | 4.2 | 0.5 | −17.3 (1050) | −31.4 (1500) |
| $[V_2Cl_2(bpy)_4(\mu\text{-}O)]Cl_2$ | 21.1 (840) | 40.1 (1560) | 9.7 (540) | 17.5 (780) | 5.6 | −17.0 (900) | −32.6 (2340) | −47.0 (3360) |

[a] Observed $^1$H NMR chemical shifts in $CD_3OD$ at 23 °C from TMS. [b] (A) and (B) refer to phen or bpy (A) and phen or bpy (B), respectively. [c] Overlapping with other signals.

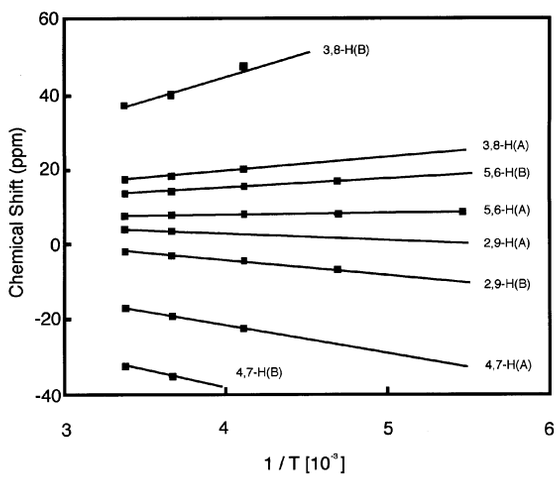


**Fig. 4** The temperature dependence of the $^1$H NMR chemical shifts for **1**.

temperature dependence of the $^1$H NMR chemical shifts are plotted against $1/T$ in Fig. 4. The apparent straight lines demonstrate that all eight $^1$H NMR signals can be attributed to the same compound over the temperature range studied, indicative of the main species being the oxo-bridged dinuclear complex.

In order to assign each of the four $^1$H NMR signals to phen protons, analogous dinuclear vanadium(III) complexes were prepared using phen derivatives and their $^1$H NMR spectra were measured in $CD_3OD$ at 23 °C (Fig. 5). All the spectral patterns are quite similar to each other, indicating that these dinuclear vanadium(III) complexes have same coordination environments. The spectra were compared with those of **1**. In the spectrum of the 4,7-$Me_2$phen complex, two signals which appear at −17.2 and −32.7 ppm for **1** disappear and two new peaks due to the methyl groups in the 4 and 7 positions appear at 50.4 and 32.9 ppm. For the 3,4,7,8-$Me_4$phen complex, four signals seen at 37.2, 17.5, −17.2 and −32.7 ppm for **1** disappear and four new resonances appear at 49.5, 31.9, −10.5 and −25.6 ppm. Furthermore, in the spectrum of the 5,6-$Me_2$phen complex, two peaks due to the Me groups were observed at −1.7 and −7.3 ppm, while the two signals observed at 13.6 and 7.5 ppm in the specrum of **1** disappeared. Similarly, the $^1$H NMR signals due to the the 2 and 9 position of phen were examined using a 2,9-phen compound. On the basis of these results, all the $^1$H NMR signals were assigned and are listed in Table 6. $^1$H NMR signals for the methyl-substituted complexes were observed in the range 45 to −55 ppm, similarly to $[V_4O_2(O_2CEt)_7(bpy)_2](ClO_4)$.[18] The resonances display the alternating shift pattern characteristic of contact shifts resulting from spin delocalization onto the ligand *via* a π-delocalization pathway.[18,24] These patterns are similar to those found for $[V_4O_2(O_2CEt)_7(bpy)_2](ClO_4)$.[18]

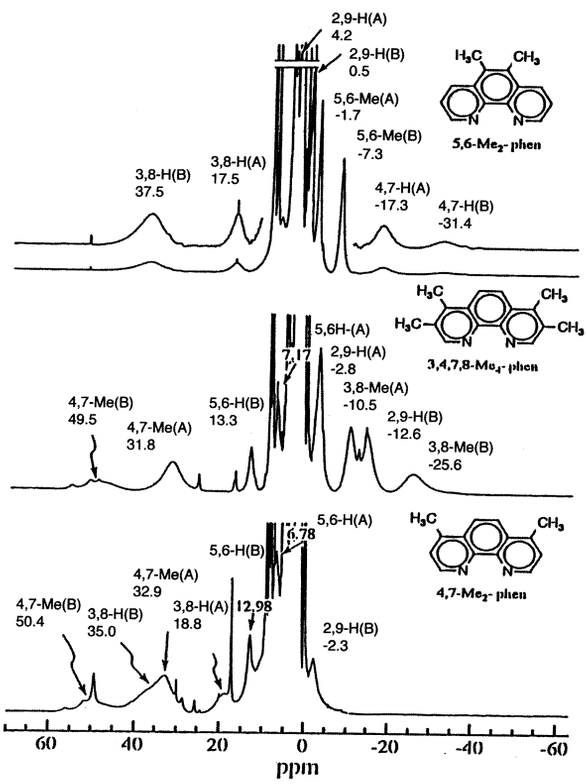


**Fig. 5** $^1$H NMR signals of analogous dinuclear vanadium(III) complexes with phen analogue measured in $CD_3OD$ at 23 °C

On the basis of this results, an analogous dinuclear vanadium(III) complex, $[V_2Cl_2(bpy)_4(\mu\text{-}O)]Cl_2$ (**5**) (bpy = 2,2′-bipyridine), was synthesized and its $^1$H NMR spectrum was measured. The crystal structure of **5**, which was obtained from preparations in water, has already been reported.[6] Similar to dinuclear vanadium(III) phen complexes, **5** provides a oxo-bridged dinuclear structure with a *cis*-bpy and *trans*-bpy. Eight broad $^1$H NMR signals were found in the spectrum of **5** at 23 °C in $CD_3OD$ 45 to −55 ppm, as was the case for **1**.[18] These $^1$H NMR signals can be classified into two types [(A) and (B)], as for phen. Plotting the temperature dependence of the $^1$H NMR chemical shifts against $1/T$ also gives apparently linear correlations, showing that the main species is an oxo-bridged dinuclear complex. On the basis of the data for the dinuclear vanadium(III) phen complexes, all eight $^1$H NMR signals of **5** were assigned and the chemical shift values are listed in Table 6. All of the $^1$H NMR signals due to coordinated bpy in the spectrum of **5** are shifted. The coordinated bpy resonances

display a contact shifted pattern similar to that seen for $[V_4O_2(O_2CEt)_7(bpy)_2](ClO_4)$.[18]

In conclusion, the $^1H$ NMR signals of antiferromagnetic oxo-bridged dinuclear vanadium(III) complexes with bidentate N-donor ligands can be readily observed and behavior in solution as well as in the dinuclear structure can be examined.

## Acknowledgements

This research was supported by a Grant-in-Aid for scientific research on Priority Area "Metal-assembled complexes" (no. 10149101) from the Ministry of Education, Science and Culture, Japan.

## References and notes

1 (*a*) G. Christou, D. Heinrich, J. K. Money, J. R. Rambo, J. C. Huffman and K. Folting, *Polyhedron*, 1989, **8**, 1723; (*b*) M. R. Bond, R. S. Czernuszewicz, B. C. Dave, Q. Yan, M. Mohan, R. Verastegue and C. J. Carrano, *Inorg. Chem.*, 1995, **34**, 5857.
2 R. S. Czernuszewicz, Q. Yan, M. R. Bond and C. J. Carrano, *Inorg. Chem.*, 1994, **33**, 6116.
3 (*a*) K. Kanamori, M. Teraoka, H. Maeda and K. Okamoto, *Chem. Lett.*, 1993, 1731; (*b*) K. Kanamori, E. Kameda, T. Kabetani, T. Suemoto, K. Okamoto and S. Kaizaki, *Bull. Chem. Soc. Jpn.*, 1995, **68**, 2581; (*c*) P. Chandrasekhar and P. H. Bird, *Inorg. Chem.*, 1984, **23**, 3677; (*d*) Y. Zhang and R. H. Holm, *Inorg. Chem.*, 1990, **29**, 911; (*e*) K. Wieghardt, M. Koppen, B. Nuber and J. Weiss, *J. Chem. Soc., Chem. Commun.*, 1986, 1530; (*f*) C. J. Carrano, R. Verastgue and M. R. Bond, *Inorg. Chem.*, 1993, **32**, 3589; (*g*) M. Koeppen, G. Fresen, K. Wiehghardt, R. M. Llusar and M. Nuber, *Inorg. Chem.*, 1988, **27**, 721.
4 P. Knopp, K. Wieghardt, B. Nuber, J. Weiss and W. S. Sheldrick, *Inorg. Chem.*, 1990, **29**, 363.
5 T. Otieno, M. R. Bond, L. M. Mokry, R. B. Walter and C. J. Carrano, *Chem. Commun.*, 1996, 37.
6 S. G. Brand, N. Edelstein, C. J. Hawkins, G. Shalimoff, M. R. Snow and R. T. Tiekink, *Inorg. Chem.*, 1990, **29**, 434.
7 J. K. Money, K. Floting, J. C. Huffman and G. Christou, *Inorg. Chem.*, 1987, **26**, 944.
8 N. S. Dean, S. L. Bartley, W. E. Streib, E. B. Lobkovsky and G. Christou, *Inorg. Chem.*, 1995, **34**, 1608.
9 N. S. Dean, F. K. E. Lobkovsky and G. Christou, *Angew. Chem., Int. Ed. Engl.*, 1993, **32**, 594.
10 K. Wieghardt, U. Bossek, K. Volckmar, W. Swiridoff and J. Weiss, *Inorg. Chem.*, 1984, **23**, 1387.
11 P. Knopp and K. Wieghardt, *Inorg. Chem.*, 1991, **30**, 4061.
12 F. A. Cotton, G. E. Lewis and G. N. Mott, *Inorg. Chem.*, 1982, **21**, 3127.
13 F. A. Cotton, G. E. Lewis and G. N. Mott, *Inorg. Chem.*, 1982, **21**, 3316.
14 F. A. Cotton, M. W. Extine, L. R. Falvello, D. B. Lewis, G. E. Lewis, C. A. Murillo, W. Schwotzer, M. Tomas and J. M. Troup, *Inorg. Chem.*, 1986, **25**, 3505.
15 S. L. Castro, W. E. Streib, J.-S. Sun and G. Christou, *Inorg. Chem.*, 1996, **35**, 4462.
16 H. Kumagai and S. Kitagawa, *Chem. Lett.*, 1996, 471.
17 S. L. Castro, Z. Sun, J. C. Bollinger, D. N. Hendrickson and G. Christou, *J. Chem. Soc., Chem. Commun.*, 1995, 2517.
18 S. L. Castro, Z. Sun, C. M. Grant, J. C. Bollinger, D. N. Hendrickson and G. Christou, *J. Am. Chem. Soc.*, 1998, **120**, 2365.
19 R. H. Holm and J. P. Donahue, *Polyhedron*, 1993, **12**, 571.
20 R. H. Holm, *Chem. Rev.*, 1987, **87**, 1401.
21 M. Mazzanti, C. Floriani, A. Chiesi-Villa and C. Guastini, *Inorg. Chem.*, 1986, **25**, 4158.
22 S. Gambarotta, M. Mazzanti, C. Floriani, A. Chiesi-Villa and C. Guastini, *J. Chem. Soc., Chem. Commun.*, 1985, 829.
23 M. Maekawa, S. Kitagawa, M. Munakata and H. Masuda, *Inorg. Chem.*, 1989, **28**, 1904.
24 G. N. La Mar, ed., in *NMR of Paramagnetic Molecules*, Academic Press, New York, 1973.
25 I. Bertini and C. Luchinat, *Coord. Chem. Rev.*, 1996, **150**, 1.
26 K. Kanamori, Y. Ookubo, K. Ino, K. Kawai and H. Michibata, *Inorg. Chem.*, 1991, **30**, 3832.
27 K. Kanamori, J. Kumada, M. Yamamoto, T. Okayasu and K. Okamoto, *Bull. Chem. Soc. Jpn.*, 1995, **68**, 3445.
28 N. S. Dean, L. M. Mokry, M. R. Bond, C. J. O'Connor and C. J. Carrano, *Inorg. Chem.*, 1996, **35**, 3541.
29 J. A. Jensen and G. S. Girolami, *Inorg. Chem.*, 1989, **28**, 2114.
30 E. Kurras, *Naturwissenschaften*, 1959, **46**, 171.
31 A. Bencini and D. Gatteschi, in *Transition Metal Chemistry*; ed. G. A. Melson and B. N. Figgis, Marcel Dekker, New York, 1982, vol. 8.
32 G. M. Sheldrick, in *Crystallographic Computing 3*, Oxford University Press, London, 1985.
33 H. Toftlund, S. Larsen and K. S. Murray, *Inorg. Chem.*, 1991, **30**, 3964.
34 S. Dutta, P. Basu and A. Chakravorty, *Inorg. Chem.*, 1993, **32**, 5343.
35 J. Chakravarty, S. Dutta and A. Chakravorty, *J. Chem. Soc., Dalton Trans.*, 1993, 2857.
36 A. Kojima, K. Okazaki, S. Ooi and S. Kazuo, *Inorg. Chem.*, 1983, **22**, 1168.
37 M. Nishizawa, K. Hirotsu, S. Ooi and K. Saito, *J. Chem. Soc., Chem. Commun.*, 1979, 707.
38 J.-P. Launay, Y. Jeannin and M. Daoudi, *Inorg. Chem.*, 1985, **24**, 1052.
39 J. C. Pessoa, J. A. L. Silva, L. Vilas-Boa, P. O'Brien and P. Thornton, *J. Chem. Soc., Dalton Trans.*, 1992, 1745.
40 H. Schmidt, M. Bashirpoor and D. Rehder, *J. Chem. Soc., Dalton Trans.*, 1996, 3865.
41 $V_2O_3C_{40}N_{12}Cl_4H_{36}$, $M$ = 976.50, crystal size, 0.6 × 0.4 × 0.1 mm$^3$; monoclinic, $a$ = 35.158(8), $b$ = 16.984(4), $c$ = 20.180(8) Å, $\beta$ = 112.09(3)°, $V$ = 11165(5) Å$^3$, space group $C2/c$, $Z$ = 8, $D_c$ = 1.162 g cm$^{-3}$, $\mu$(Mo-K$\alpha$) = 5.63 cm$^{-1}$, no. of reflections measured = 13273 ($R_{int}$ = 0.013), no. observations = 4786 [$I > 3.00\sigma(I)$], $R$ ($Rw$) = 0.103 (0.167). CCDC reference number 167775. See http://www.rsc.org/suppdata/dt/b1/b106517n/ for crystallographic data in CIF or other electronic format.
42 J. R. Philbrow, in *Transition Ion Electron Paramagnetic Resonance*, Oxford University Press, New York, 1990.
43 A. Abragam and B. Bleaney, in *Electron Paramagnetic Resonance of Transition ions*, Clarendon, New York, 1970.
44 F. A. Cotton and J. Lu, *Inorg. Chem.*, 1995, **34**, 2639.
45 J. Lambe and C. Kikuchi, *Phys. Rev.*, 1960, **118**, 71.
46 T. W. Newton and F. B. Baker, *J. Phys. Chem.*, 1964, **68**, 228.
47 K. Kanamori, K. Ino, H. Maeda, K. Miyazaki, M. Fukagawa, J. Kumada, T. Eguchi and K. Okamoto, *Inorg. Chem.*, 1994, **33**, 5547.
48 The contact shift of *trans*-phen is expected to be larger than those of *cis*-phen.